Current-noise-power spectra of amorphous silicon thin-film transistors

J. M. Boudry and L. E. Antonuk
Department of Radiation Oncology, University of Michigan, Ann Arbor, Michigan 48109

(Received 23 December 1993; accepted for publication 29 April 1994)

Current-noise-power spectra of thin-film transistors (TFTs) fabricated from hydrogenated amorphous silicon were measured. TFTs with aspect ratios ranging from 1:1 to 16:1 were examined in both the conducting and nonconducting modes. In the conducting mode, the noise levels could be predicted to within an order of magnitude by theories developed for crystalline metal-oxide field-effect transistors. In the nonconducting mode, the noise was found to scale with the TFT leakage current in a power-law fashion.

I. INTRODUCTION

Thin-film transistors (TFTs) fabricated from hydrogenated amorphous silicon (a-Si:H) are an important component of large area, pixelated arrays used for imaging applications. For both image display and image capture applications, the TFTs act as switching components and allow for the addressing of individual array pixels. A summary of imaging applications which incorporate a-Si:H arrays has been reported by Street.[1] A specific application under development by our collaboration is the use of two-dimensional, photosensitive a-Si:H arrays for x-ray imaging.[2] Each pixel of these arrays consists of an a-Si:H photodiode sensor connected in series with an a-Si:H TFT. The sensors detect incident x rays indirectly by means of an overlaying x-ray converter such as a phosphor screen. Manipulation of the TFT gate voltage renders the TFT conducting (positive gate voltage) or nonconducting (negative gate voltage). This allows for the integration of charge created in the sensor due to incoming light photons (TFT nonconducting) and the subsequent readout by external electronics of the integrated charge (TFT conducting). Presently, x-ray images of human anatomical features using (23×25) cm^2 a-Si:H arrays with (512×560) pixels have been demonstrated.[3]

The present use and future potential of a-Si:H arrays for x ray and other imaging applications warrants a study of the noise properties of a-Si:H TFTs. This paper presents current-noise-power spectrum measurements of a-Si:H TFTs fabricated with the same design and deposition parameters as those used for x-ray imaging arrays. The measurements were carried out for different size TFTs at various operating voltages. The TFT sizes and voltages were chosen so as to correspond to those currently used for x-ray imaging arrays.

Previous power spectra measurements of a-Si:H TFTs of similar construction have been presented by Cho *et al.*[4] They measured the flicker noise of a TFT in the conducting mode. This study presents measurements of both the flicker and thermal noise in the conducting mode and the flicker noise in the nonconducting mode. In addition, the magnitude of the flicker and thermal noise levels in the conducting mode are compared with theoretical predictions obtained for crystalline metal-oxide field-effect transistors (MOSFETs), and a power-law relationship between TFT leakage current and flicker noise level is empirically obtained in the nonconducting mode.

II. DESCRIPTION OF THIN-FILM TRANSISTOR

The TFTs that were studied had an inverted staggered structure which is schematically illustrated in Fig. 1. The width W and length L are also indicated in the figure. The length of the TFTs was constant and equal to 15 μm while the widths ranged from 15 to 240 μm. The ratio of the width to the length is termed the aspect ratio W/L. TFTs with W/L values of 16:1, 8:1, 4:1, and 1:1 were examined.

The TFT shown in Fig. 1 is a single-carrier device. This is facilitated by the n-type doped layers at the source and drain contacts which permit electron conduction through the a-Si:H layer, but block hole conduction. For positive gate voltages, an electron layer is induced in the a-Si:H channel and conduction occurs. This is termed the conduction or "on" mode. For negative gate voltages, hole conduction through the a-Si:H channel is minimal due to the low hole mobility and the n-type doped blocking layers.[5] This is termed the nonconducting or "off" mode. Typical order of magnitude on and off currents for these TFTs are 1 μA and 0.1 pA, respectively, giving an on-to-off current ratio of order 10^7.

Measurements of the operational characteristics were performed for the four different aspect ratio TFTs whose noise was characterized in the conducting mode. The transfer and output characteristics of the 4:1 aspect ratio TFT are shown in Fig. 2. The transfer characteristic [Fig. 2(a)] shows the drain-source current i_{ds} versus the gate voltage V_g for several values of the drain-source voltage V_{ds}. In this plot, both the nonconducting and conducting modes of the TFT are revealed. For negative V_g, i_{ds} ranges from ~3 to 100 fA and reaches ~1 μA for large positive V_g. A transition between the conducting and nonconducting modes occurs for V_g ranging from ~0 to 3 V. The characteristic gate voltage for which this transition occurs is called the threshold voltage V_T. Measured values of V_T for the four aspect ratio TFTs are listed in Table I. The output characteristic shown in Fig. 2(b) is a plot of i_{ds} versus V_{ds} for different values of V_g. The V_g values were such that the TFT was in the conducting mode. Output characteristics were measured for each of the different aspect ratio TFTs for V_g and V_{ds} ranging as in Fig. 2(b). For these voltages, i_{ds} could be predicted to within 17% for each aspect ratio TFT by using the following equation developed for crystalline MOSFETs.[6]

0021-8979/94/76(4)/2529/6/$6.00
© 1994 American Institute of Physics

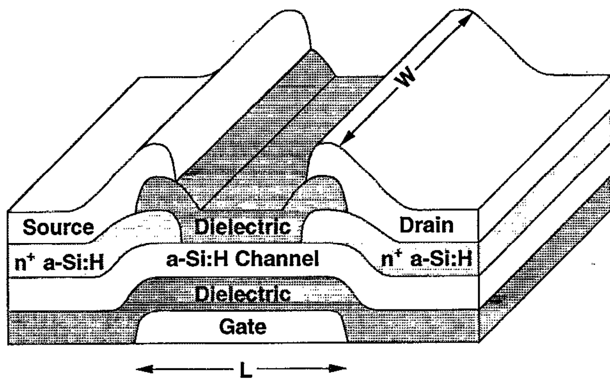

FIG. 1. Schematic diagram showing the general design of the a-Si:H TFTs used for this study. The gate, source, and drain layers consist of chrome and the dielectric layers are amorphous silicon nitride (a-Si_3N_4:H).

$$i_{ds}=\mu\Gamma(W/L)\left[(V_g-V_T)V_{ds}-\frac{V_{ds}^2}{2}\right]. \quad (1)$$

In this expression, Γ is the capacitance per unit area formed between the a-Si:H conducting channel and the gate contact (~20 nf/cm^2) and μ is the mobility of electrons in a-Si:H (measured values listed in Table I). For small V_{ds} ($V_{ds}\ll V_g-V_T$), i_{ds} varies linearly with V_{ds} and the TFT is said to be in the linear region of operation. For $V_{ds}\gg(V_g-V_T)$, V_{ds} is set equal to (V_g-V_T) in Eq. (1) and i_{ds} is independent of V_{ds}. This is termed the saturation region. Both the linear and saturation regions are observed in Fig. 2(b).

III. NOISE MEASUREMENT TECHNIQUE

Since the drain-source current is integrated by external electronics in order to determine the imaging signal, it is of interest to measure the noise characteristics of i_{ds}. The noise characteristics were quantified in terms of current-noise-power spectra. In general, a noise power spectrum gives information pertaining to the frequency content of a noise process. It is a plot of the power density of a randomly fluctuating quantity versus frequency. The current-noise-power density of the drain-source current, $S_i(f)$, was determined according to the following relation

$$S_i(f)=2\,\frac{\overline{|I_T(f)|^2}}{T}, \quad (2)$$

where $|I_T(f)|$ is the magnitude of the finite Fourier transform of i_{ds} measured over a time interval, T. The bar denotes an ensemble average.[7] Power-spectra measurements were performed for different V_g, V_{ds}, and W/L.

Current-noise-power spectra of the TFTs were obtained as follows. V_g and V_{ds} were provided either by batteries or by a voltage source/picoammeter (Hewlett Packard 4140B). Use of the HP-4140B provided the additional capabilities of measuring i_{ds} and allowing computer control of the voltage settings. However, bandwidth limitations prevented use of the HP-4140B for power spectra measurements involving frequencies greater than ~10 Hz. For frequencies ranging

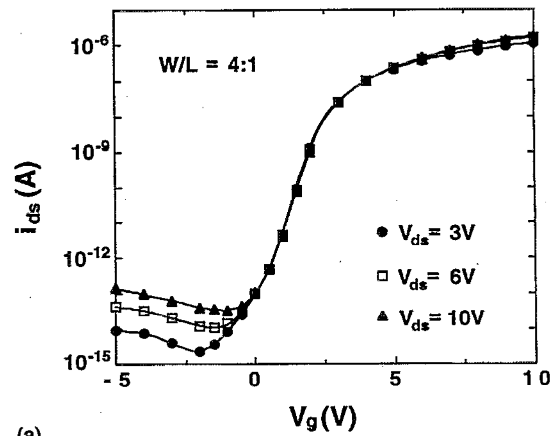

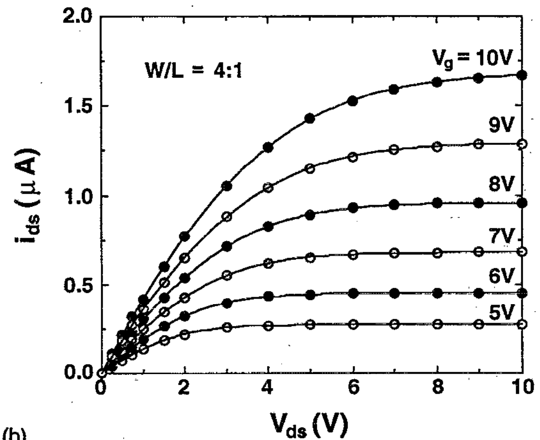

FIG. 2. (a) Transfer and (b) output characteristics of a 4:1 aspect ratio TFT. The measured threshold voltage V_T and mobility μ of the four different aspect ratio TFTs used for the conducting mode measurements are listed in Table I. The lines through the data were obtained by interpolation.

from ~10 Hz to 1 kHz, batteries were used. In order to determine $I_T(f)$, the fluctuations in i_{ds} were sampled via the amplification network shown in Fig. 3. The first stage of the network consisted of a transimpedance amplifier (Ithaco 1212) and the second stage was an ac-coupled voltage amplifier. The dc gain of the transimpedance amplifier ranged from 10^5 to 10^{10} V/A and the second stage passband gain was ~500. The voltage fluctuations after the two amplification stages were related to the drain-source current fluctuations by the gain, $G(f)$, of the amplification network. (Measurements of $G(f)$ were performed over the frequency range of interest using a function generator.) The voltage fluctua-

TABLE I. Measured mobilities and threshold voltages and calculated overlap capacitances for the various a-Si:H TFTs.

Aspect ratio W/L	Mobility μ (cm^2/V s)	Threshold voltage V_T (V)	Overlap capacitance C_{gd} (pF)
1	0.93	1.8	0.01
4	0.70	1.7	0.05
8	0.67	1.7	0.1
16	0.69	2.1	0.2

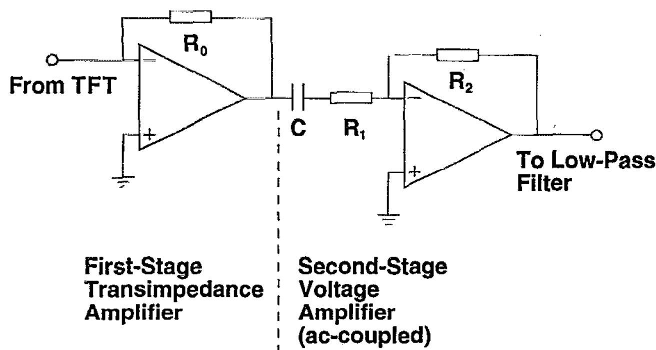

FIG. 3. Detailed diagram of the amplifying network. R_0 determined the gain of the transimpedance amplifier (10^5–10^{10} V/A). R_1, R_2, and C values were nominally 1 kΩ, 500 kΩ, and 235 μF, respectively.

tions were passed through a low-pass, antialiasing filter (Frequency Devices; 8-pole Butterworth) before being sampled by a digital oscilloscope (LeCroy 9400A). The sampling rate of the oscilloscope determined the Nyquist frequency and the low-pass filter was accordingly set to one-half of this frequency to limit aliasing. The voltage fluctuations were sampled for a temporal interval T. This is referred to as a noise wave form. After sampling at least 100 noise wave forms, a MAC II computed the current-noise-power density using Eq. (2) and $G(f)$.

For each measured power spectrum, noise wave form acquisition commenced 5 min after application of V_g and V_{ds}. This was to allow for i_{ds} and the noise to stabilize sufficiently. After the acquisition of each noise wave form, i_{ds} was measured (if the HP-4140B was used as the voltage source) and the standard deviation of the noise wave form was computed. The values of i_{ds} and the noise wave form standard deviation typically deviated 5% from their mean values for each measured power spectrum.

IV. SYSTEM CALIBRATION

The system calibration was verified by measuring the thermal noise of known resistive values. The measurement system noise was dominated by the input noise of the transimpedance amplifier, which consists of a parallel current-noise-source, $i_a(f)$, and a series voltage-noise-source, $e_a(f)$. With a TFT connected to the input, the circuit shown in Fig. 4 was used to determine the current-noise-power density at the amplifier input, $S_{in}(f)$, due to $i_a(f)$ and $e_a(f)$. R_{TFT} represents the TFT resistance. For positive gate voltages, R_{TFT} was calculated using Eq. (1). For negative gate voltages, R_{TFT} was assumed to be infinite. C_{gd} is the capacitance due to the overlap between the gate and drain contacts. (Calculated values for the different aspect ratio TFTs are listed in Table I.) $S_{in}(f)$ specifies the system noise and from standard circuit analysis is given by the following relation

$$S_{in}(f)=i_a(f)+e_a(f)\ \frac{1+(2\pi f R_{\text{TFT}}C_{gd})^2}{R_{\text{TFT}}^2}. \tag{3}$$

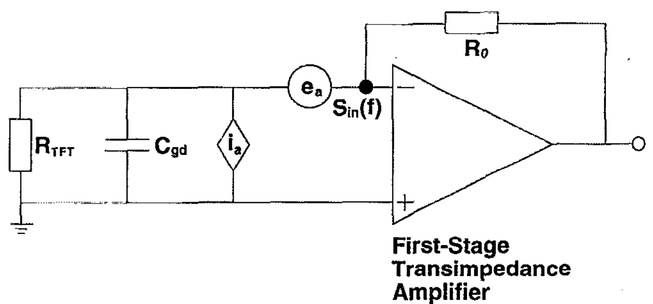

FIG. 4. Circuit used for determining the system noise with a TFT connected at the input. Calculated capacitance values for the four different aspect ratios are listed in Table I.

The system noise was typically 1–2 orders of magnitude below the measured TFT noise and was subtracted from each measured power spectrum.

V. RESULTS: CONDUCTING MODE (POSITIVE V_g)

A. Measured power spectra

Figure 5 shows measurements of power spectra for the 4:1 aspect ratio TFT for various V_{ds}. Over the frequency range of $\sim 10^{-1}$–10^3 Hz, two noise components are present. The first, displaying a $1/f^{\gamma}$ ($\gamma\approx 1$) dependence, is the well-known flicker noise. The second is independent of frequency and is called thermal noise as it is due to the thermal fluctuation of electrons in the conducting channel of the TFT.

Both the thermal and flicker noise components were measured as a function of V_g, V_{ds}, and W/L. The flicker noise component was characterized by power spectra measurements out to 10 Hz rather than over the whole frequency range ($\sim 10^{-1}$–10^3 Hz). The thermal noise component was determined by power-spectra measurements over the entire frequency range. Measurement results of the flicker and thermal noise levels as a function of V_g, V_{ds}, and W/L are

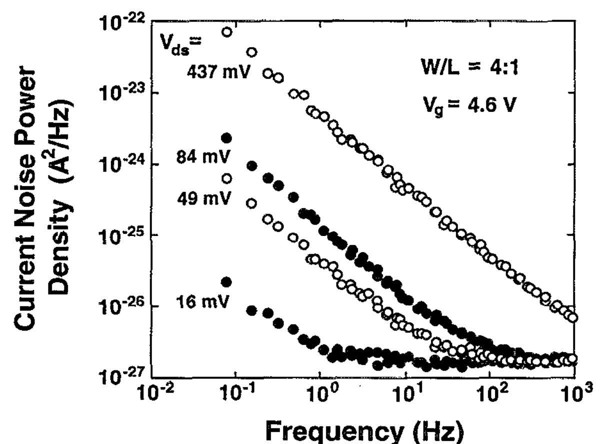

FIG. 5. Measured power spectra for the 4:1 aspect ratio TFT in the conducting mode. For lower V_{ds}, both a flicker and thermal noise component are observed. As V_{ds} increases, the flicker component dominates over the entire frequency range. The thermal component is observed to be independent of V_{ds}.

given below and compared with theoretical predictions. For these comparisons, possible shifts in the threshold voltage due to bias stress were neglected.[8]

B. Flicker noise component

1. Theory

The formulation presented here is based on previous work performed for crystalline devices. Let $S_{fl}(f)$ denote the flicker noise component of the current-noise-power density of a crystalline MOSFET in the conducting mode. For arbitrary V_{ds}, Van der Ziel[9] derived the following expression for $S_{fl}(f)$

$$S_{fl}(f)=\frac{q^2\mu^2(W/L)^2}{WL}S_n(f)\frac{V_g-V_T-\frac{V_{ds}}{2}}{V_g-V_T}V_{ds}^2. \quad (4)$$

In this expression, $S_n(f)$ is the noise-power density of the charge carriers per unit area (for $V_{ds} \ll V_g-V_T$) and q is the magnitude of the electron charge. Equation (4) was obtained under the assumption that the origin of the flicker noise is the random capture and emission of charge carriers by localized states in the oxide layer of the MOSFET. The interaction mechanism is quantum-mechanical tunneling mediated by surface states. From Klaassen,[10] $S_n(f)$ is

$$S_n(f)=\frac{\alpha n}{f}, \quad (5)$$

where n is the number of free charge carriers per unit area and α is a number which is assumed to be nearly constant.[10,11] Using the relation[6]

$$qn=\Gamma(V_g-V_T), \quad (6)$$

Eq. (4) can be rewritten as

$$S_{fl}(f)=\frac{\alpha q\mu^2\Gamma(W/L)^2}{(WL)f}\left(V_g-V_T-\frac{V_{ds}}{2}\right)V_{ds}^2. \quad (7)$$

Equation (7) specifies the magnitude of the flicker noise and is valid for arbitrary V_{ds}. In saturation, V_{ds} is set equal to (V_g-V_T). By comparing the measured flicker noise in the conducting mode with Eq. (7), the value of α and its dependence on V_g and V_{ds} can be determined.

2. Measurements and comparison with theory

The flicker noise component was measured for V_g ranging from 5 to 10 V and for V_{ds} from 0.4 to 10 V. These voltages span both the linear and saturation regions of TFT operation and are representative of those encountered in x-ray imaging applications. The flicker noise was quantified by fitting the measured power spectra with the function FC_{on}/f^{γ}. The exponent γ, which specifies the frequency dependence, had an average value of 1.03±0.05 for the measured power spectra. The coefficient FC_{on} is termed the flicker coefficient in the conducting mode and it specifies the magnitude of the flicker noise component. Measurements of FC_{on} for the 4:1 aspect ratio TFT are plotted in Fig. 6. Similar measurements were carried out for the other aspect ratio TFTs. The dependence of FC_{on} on V_g and V_{ds}, when plotted on logarithmic axes, is analogous to an output characteristic.

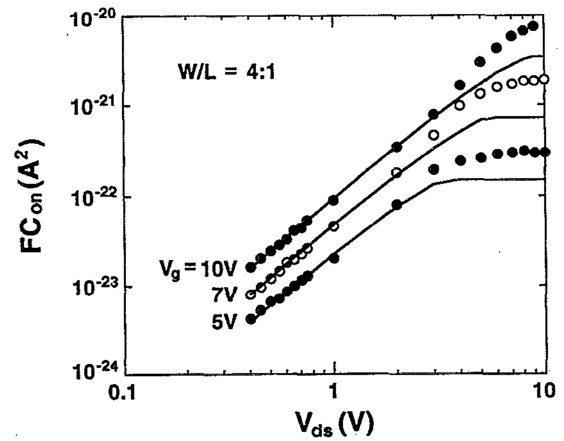

FIG. 6. Measured flicker coefficients for the 4:1 aspect ratio TFT in the conducting mode for various V_g and V_{ds}. The lines through the data are calculated using Eq. (7) with $\alpha=2.9\times10^{-3}$, 3.4×10^{-3}, and 4.2×10^{-3} for V_g=5, 7, and 10 V, respectively.

In the linear region the flicker coefficients display a power-law relationship with V_{ds} and saturate in the TFT saturation region.

The functional dependence of the measured flicker coefficients on V_g and V_{ds} was determined in the linear and saturation regions from the slopes of power-law fits to the data. These calculations assumed that α is independent of V_g and V_{ds}. In the linear and saturation regions, the corresponding flicker coefficients, $(FC_{on})_{lin}$ and $(FC_{on})_{sat}$, obtained from Eq. (7) are

$$(FC_{on})_{lin}=\frac{\alpha q\mu^2\Gamma(W/L)^2}{WL}(V_g-V_T)V_{ds}^2, \quad (8a)$$

$$(FC_{on})_{sat}=\frac{\alpha q\mu^2\Gamma(W/L)^2}{2WL}(V_g-V_T)^3. \quad (8b)$$

In the linear region, the dependence of $(FC_{on})_{lin}$ on V_{ds} and (V_g-V_T) was determined for $5\leq V_g\leq10$ V and $V_{ds}\leq1$ V for the four different aspect ratio TFTs. The dependence of $(FC_{on})_{sat}$ on (V_g-V_T) was determined for each aspect ratio TFT with V_{ds} equal to 9 and 10 V and $5\leq V_g\leq10$ V. The calculated slope values were averaged over the four aspect ratio TFT measurements. $(FC_{on})_{lin}$ was found to depend on V_{ds} and (V_g-V_T) raised to the 1.85±0.10 and 1.31±0.23 powers, respectively. $(FC_{on})_{sat}$ depended on (V_g-V_T) raised to the 3.36±0.25 power. These values are in reasonable agreement with Eqs. (8a) and (8b). Figure 6 also illustrates that FC_{on} shows little or no dependence on V_{ds} in the saturation region as predicted by Eq. (8b).

The value of α was determined by comparing the measured FC_{on} values with those predicted by Eq. (7) with α set to unity. The ratio of FC_{on} to these predicted values, $FC_{\alpha=1}$, is shown in Fig. 7 for the 4:1 TFT. It is apparent that the actual value of α ranges from $\sim3\times10^{-3}$ to 1×10^{-2} for the range of V_g and V_{ds} studied. For a given V_g, α is relatively constant for $V_{ds}\leq2$ V and then begins to increase with V_{ds}. The V_g=5 V data show saturation at large V_{ds} but this is not as evident for the larger gate voltages. The behavior of α

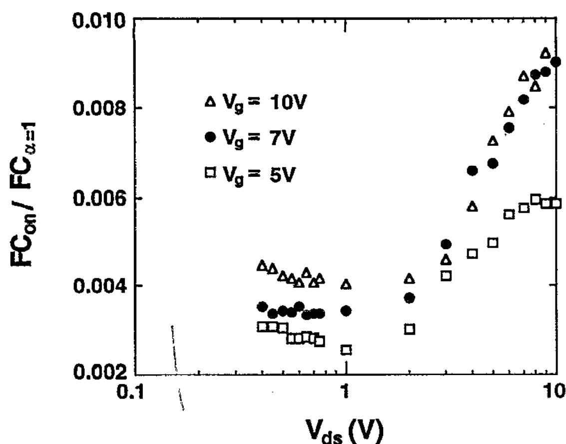

FIG. 7. Ratio of the measured flicker coefficient to the value predicted using Eq. (7) (with $\alpha=1$) as a function of V_{ds} for various V_g. These results correspond to the 4:1 aspect ratio TFT.

with V_g and V_{ds} was similar for the other aspect ratio TFTs. For $V_{ds} \leqslant 2$ V, α ranged from $\sim 3\times 10^{-3}$ to 5×10^{-3}. Thus, in this region, Eq. (7) with α set equal to 4×10^{-3} can be used with reasonable accuracy in predicting $FC_{\rm on}$. For $V_{ds}>2$ V, α set equal to 6×10^{-3} will give order of magnitude accuracy.

C. Thermal noise component

The expected magnitude of the thermal noise N_{th} of a crystalline MOSFET at temperature T is[12]

$$N_{th}=\beta 4kT\mu\Gamma(W/L)(V_g-V_T), \tag{9}$$

where k is Boltzmann's constant and β is a number ranging from approximately one ($V_{ds} \ll V_g - V_T$) to two-thirds ($V_{ds} \gg V_g - V_T$). Measurements of the thermal noise component magnitude for the four aspect ratio TFTs as a function of gate voltage are shown in Fig. 8. The measurements were performed for low V_{ds} ($\sim$16 mV) as the flicker noise component dominated over the entire frequency range for higher V_{ds}. The lines shown in Fig. 8 were calculated from Eq. (9) and show reasonable agreement with the measured values, differing from 10% to 40%. In Fig. 5, the power spectra reveal the thermal noise to be independent of V_{ds} (in the linear region). This is also in agreement with Eq. (9).

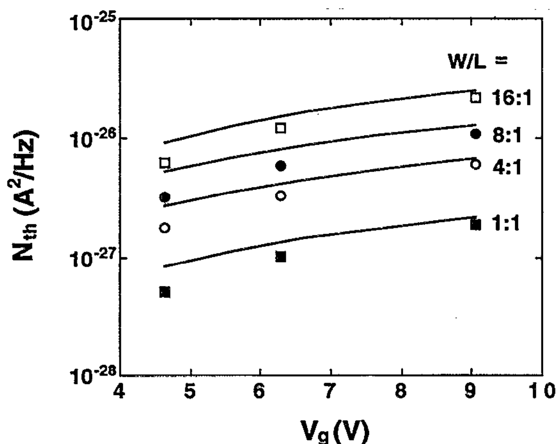

FIG. 8. Magnitude of the thermal noise component for the four different aspect ratio TFTs as a function of gate voltage. V_{ds} was $\sim$16 mV for each measurement. The lines were calculated using Eq. (9).

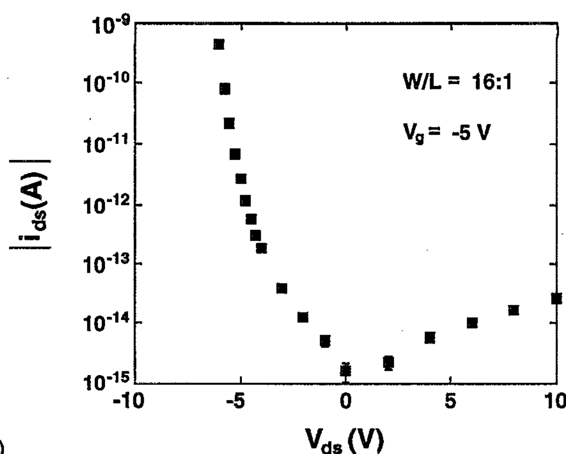

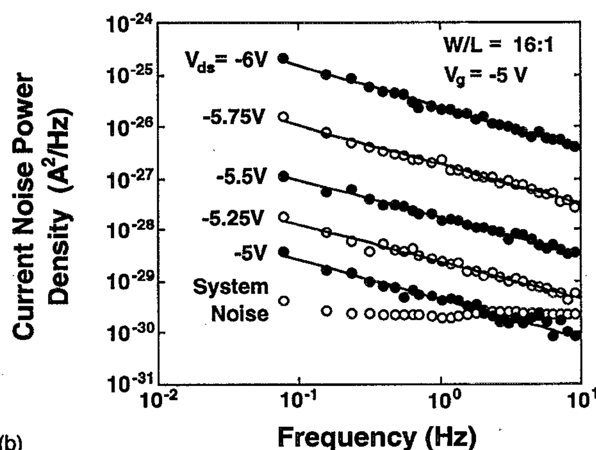

FIG. 9. (a) Magnitude of the drain-source current for $V_g=-5$ V and (b) associated power spectra for a 16:1 TFT. Lines through the power spectra data represent fits of the form $FC_{\rm off}/f^{\delta}$. On average, $\delta=0.77\pm 0.06$.

VI. RESULTS: NONCONDUCTING MODE (NEGATIVE V_g)

For negative V_g, the TFT noise could not be resolved from the measurement system noise unless V_{ds} was approximately equal to or more negative than V_g. In these configurations, i_{ds} was sufficiently large so that a flicker noise component could be measured. (The flicker noise of a device is often proportional to the square of the current through the device.[9]) Figure 9 shows the magnitude of i_{ds} and the corresponding power spectra measurements for a 16:1 TFT with $V_g=-5$ V. The magnitude of i_{ds} and the power spectra are seen to increase dramatically as V_{ds} becomes more negative than V_g.

Similar measurements to those shown in Fig. 9 were carried out for a total of eight different TFTs (two TFTs were examined for each aspect ratio). For each TFT, three V_g val-

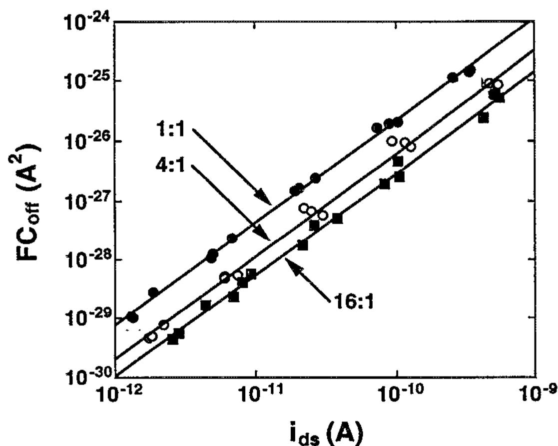

FIG. 10. $FC_{\rm off}$ for a 1:1 (●), 4:1 (○), and 16:1 (■) TFT as a function of i_{ds}. For clarity, the 8:1 aspect ratio data are omitted but showed the same power-law behavior and generally fell between the 4:1 and 16:1 data.

ues were examined ranging from -2 to -10 V. For each V_g, five V_{ds} settings were used ranging from V_g to 2 V less than V_g. All of the measured power spectra were of the form $FC_{\rm off}/f^\delta$. The value of δ was relatively independent of V_g, V_{ds}, and W/L and had an average value of 0.77 ± 0.06, which is slightly smaller than what is usually reported for flicker noise.[13] The flicker coefficient in the nonconducting mode, $FC_{\rm off}$, depended on i_{ds} in a power-law fashion. This is displayed in Fig. 10 for three different aspect ratio TFTs. The lines represent power-law fits. On average, $FC_{\rm off}$ depended on i_{ds} raised to the 1.73 ± 0.09 power. The data in Fig. 10 also indicate that, for a given i_{ds}, $FC_{\rm off}$ tends to increase for decreasing W/L. This dependence roughly goes as $(W/L)^{-0.75}$ and is weak in comparison to the i_{ds} dependence. The empirical fits shown in Fig. 10 make it possible to estimate the flicker noise component of a TFT in the nonconducting mode if i_{ds} is known.

For each TFT, it was generally observed that $FC_{\rm off}$ depended on the difference between V_g and V_{ds}, rather than their absolute values. This follows from the observation that i_{ds} was also dependent on this difference.

VII. CONCLUSIONS

The current-noise-power spectra of different aspect ratio a-Si:H TFTs were measured for various voltage settings. For gate and drain-source voltages ranging from ~5 to 10 and 0 to 10 V, respectively, the power spectra over the frequency range of 10^{-1}–10^3 Hz were composed primarily of flicker and thermal noise components. The magnitude of these two components could be predicted with reasonable accuracy using expressions derived for crystalline devices of similar structure. For negative gate voltages ($-10\leq V_g\leq-2$ V), power spectra with a $1/f^\delta$ ($\delta=0.77\pm0.06$) dependence were measured. The magnitude of these power spectra scaled with the drain-source current raised to the 1.73 ± 0.09 power and showed a relatively weak dependence on aspect ratio.

The characterization of the noise-power spectra of a-Si:H TFTs at the voltage settings used in this study greatly aids in predicting their noise levels when operating on a-Si:H x-ray imaging arrays. These measurements can be extended to a-Si:H TFTs used for other applications if they are operated at similar voltage settings.

ACKNOWLEDGMENTS

This work was supported by National Institutes of Health Grant No. 1-R01-CA 56135-01. The authors wish to thank Robert Street and Richard Weisfield at Xerox, PARC for supplying the devices used in this study.

[1] R. A. Street, MRS Bull. **17**, 70 (1992).
[2] L. E. Antonuk, J. Boudry, W. Huang, D. L. McShan, E. J. Morton, J. Yorkston, M. J. Longo, and R. A. Street, Med. Phys. **19**, 1455 (1992).
[3] L. E. Antonuk, J. Yorkston, W. Huang, J. Boudry, E. J. Morton, and R. A. Street, SPIE **1896**, 18 (1993).
[4] G. Cho, J. S. Drewery, I. Fujieda, T. Jing, S. N. Kaplan, V. Perez-Mendez, S. Qureshi, D. Wildermuth, and R. A. Street, Mater. Res. Soc. Proc. **192**, 393 (1990).
[5] R. A. Street, *Hydrogenated Amorphous Silicon* (Cambridge University Press, Cambridge, 1991), p. 374.
[6] S. R. Hofstein, in *Field-Effect Transistors*, edited by J. T. Wallmark and H. Johnson (Prentice-Hall, Englewood Cliffs, NJ, 1966), Chap. 5, pp. 113–118.
[7] M. J. Buckingham, *Noise in Electronic Devices and Systems* (Ellis Horwood, West Sussex, UK, 1983), p. 32.
[8] M. J. Powell, C. van Berkel, I. D. French, and D. H. Nicholls, Appl. Phys. Lett. **51**, 1242 (1987).
[9] A. van der Ziel, Adv. Electron. Electron Phys. **49**, 225 (1979).
[10] F. M. Klaassen, IEEE Trans. Electron Devices **ED-18**, 887 (1971).
[11] More discussion on α can be found in S. Y. Pai, Ph. D. thesis, University of Minnesota, 1978; A. van der Ziel, Solid-State Electron. **17**, 110 (1974).
[12] A. G. Jordan and N. E. Jordan, IEEE Trans. Electron Devices **ED-12**, 148 (1965).
[13] F. N. Hooge, T. G. M. Kleinpenning, and L. K. J. Vandamme, Rep. Prog. Phys. **44**, 479 (1981).